ESC European Society of Cardiology

Cardiovascular Research (2024) **120**, 44–55
https://doi.org/10.1093/cvr/cvad163

Point mutations in RyR2 Ca^{2+}-binding residues of human cardiomyocytes cause cellular remodelling of cardiac excitation contraction-coupling

Yanli Xia[1†], Xiao-hua Zhang[1†], Naohiro Yamaguchi[1,2], and Martin Morad [1,2]*

[1]Cardiac Signaling Center of University of South Carolina, Medical University of South Carolina and Clemson University, 68 President Street, Bioengineering building Rm 306, Charleston, SC 29425, USA; and [2]Department of Regenerative Medicine and Cell Biology, Medical University of South Carolina, 68 President Street, Bioengineering building Rm 306, Charleston, SC 29425, USA

Received 31 January 2023; revised 17 July 2023; accepted 26 September 2023; online publish-ahead-of-print 27 October 2023

Time of primary review: 41 days

Aims

CRISPR/Cas9 gene edits of cardiac ryanodine receptor (RyR2) in human-induced pluripotent stem cell derived cardiomyocytes (hiPSC-CMs) provide a novel platform for introducing mutations in RyR2 Ca^{2+}-binding residues and examining the resulting excitation contraction (EC)-coupling remodelling consequences.

Methods and results

Ca^{2+}-signalling phenotypes of mutations in RyR2 Ca^{2+}-binding site residues associated with cardiac arrhythmia (RyR2-Q3925E) or not proven to cause cardiac pathology (RyR2-E3848A) were determined using I_{Ca}- and caffeine-triggered Ca^{2+} releases in voltage-clamped and total internal reflection fluorescence-imaged wild type and mutant cardiomyocytes infected with sarcoplasmic reticulum (SR)-targeted ER-GCaMP6 probe. (i) I_{Ca}- and caffeine-triggered Fura-2 or ER-GCaMP6 signals were suppressed, even when I_{Ca} was significantly enhanced in Q3925E and E3848A mutant cardiomyocytes; (ii) spontaneous beating (Fura-2 Ca^{2+} transients) persisted in mutant cells without the SR-release signals; (iii) while 5–20 mM caffeine failed to trigger Ca^{2+}-release in voltage-clamped mutant cells, only ∼20% to ∼70% of intact myocytes responded respectively to caffeine; (iv) and 20 mM caffeine transients, however, activated slowly, were delayed, and variably suppressed by 2-APB, FCCP, or ruthenium red.

Conclusion

Mutating RyR2 Ca^{2+}-binding residues, irrespective of their reported pathogenesis, suppressed both I_{Ca}- and caffeine-triggered Ca^{2+} releases, suggesting interaction between Ca^{2+}- and caffeine-binding sites. Enhanced transmembrane calcium influx and remodelling of EC-coupling pathways may underlie the persistence of spontaneous beating in Ca^{2+}-induced Ca^{2+} release-suppressed mutant myocytes.

* Corresponding author. Tel: 843-876-2400, E-mail: moradm@musc.edu
† The first two authors contributed equally to the study.

Graphical Abstract

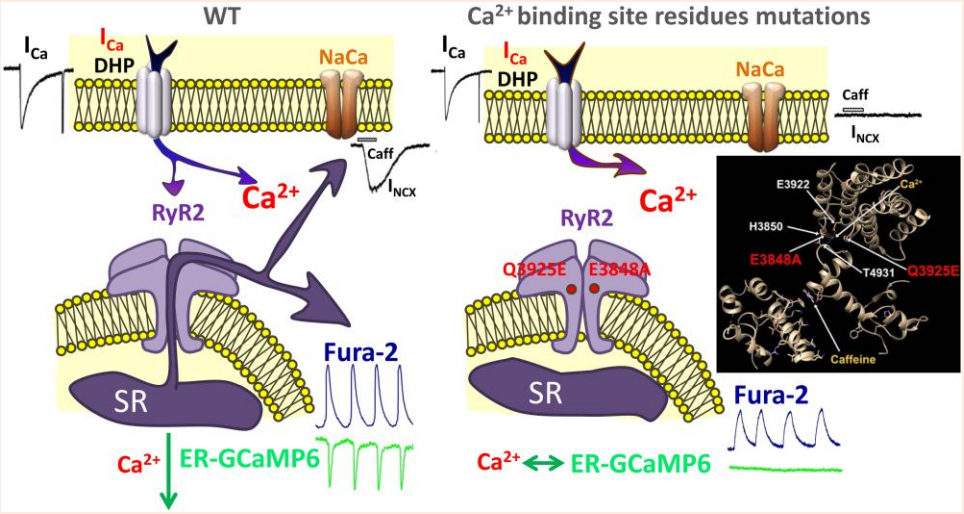

Keywords hiPSC-CMs • CRISPR/Cas9 • Q3925E and E3848A RyR2 Ca^{2+}-binding site mutations • ER-GCaMP6 SR Ca^{2+} probe • Remodelling of EC-coupling

1. Introduction

Ryanodine receptor (RyR2) is the Ca^{2+} release channel of cardiac sarcoplasmic reticulum (SR) that provides the major fraction of calcium for contraction.[1–4] Cryo-electron microscopy (EM) and three-dimensional image analysis of RyR1 have revealed the near-atomic resolution structure of the protein, identifying also the putative Ca^{2+}-, ATP-, and caffeine-binding sites.[5] Later structural analysis of RyR2 have also shown that the putative-binding sites for these three ligands were preserved in RyR2.[6] The RyR2 Ca^{2+}-binding site is formed by interaction of carboxylate side chains of residues corresponding to those of RyR1: **E3848** (3893 in RyR1) and E3922 (3967 in RyR1) in the core solenoid and the backbone carbonyl of T4931 (5001 in RyR1) in carboxyl-terminal domain. Two additional amino acids in the core solenoid, H3850 (H3895 in RyR1) and **Q3925** (3970 in RyR1), co-ordinate the Ca^{2+} sphere and serve as indirect binding residues, *Figure 1A*.[5,6] Functional studies of the recombinant mutant RyR proteins in HEK293 cells provide support for the proposed Ca^{2+}-binding site structure, showing that point mutations in all five residues alter calcium-dependent activation of RyR2.[8,9] Among the five amino acid residues of the Ca^{2+}-binding site, only glutamine substitution by glutamate, **Q3925E**, is reported to associate with arrhythmogenic pathology.[10,11] There are no reports yet that mutation of any other Ca^{2+}-binding site residues associates with CPVT1 or sudden cardiac death, but [^{3}H]ryanodine-binding assay with the recombinant RyR expressed in HEK293 cells carrying the Ca^{2+}-binding site mutation **E3848A** shows diminished Ca^{2+} activation of RyR2 and suppressed caffeine-induced Ca^{2+} release.[8,9] It has also been reported that Q3925E mutation completely abolishes store overload-induced Ca^{2+} release and reduces significantly caffeine activation of RyR2 in HEK293 cells.[12] *In silico* mutagenesis analyses based on the RyR1 Ca^{2+}-binding site, where the detailed Cryo-EM mapping is available, show that while mutations on E3848 site reduce Ca^{2+} binding, Q3925 mutations retain Ca^{2+} binding.[13,14] These results are consistent with the scheme where E3848 is direct Ca^{2+}-binding residue while Q3925 serves as an indirect binding site. Nevertheless, mutations of either residue was reported to impair Ca^{2+} activation of the recombinant RyRs expressed in HEK293 cells.[9]

Although the heterologous HEK293 cell expression system has provided considerable insight into structure/function of RyR, this platform does not express all the cardiac calcium signalling pathways of mammalian heart and as such is unlikely to show possible mutation-induced remodelling of EC-coupling. Since our earlier studies had shown remarkable similarity between Ca^{2+} signalling parameters of human stem cell derived cardiomyocytes (hiPSC-CMs) and adult or neonatal mammalian cardiomyocytes,[15,16] we chose hiPSC-CMs to investigate the effects of point mutations in RyR2 calcium-binding site, using CRSPR/Cas9 gene editing. We compared the effects of two specific point mutations in the calcium-binding pocket on cardiac EC-coupling, one associated with sudden cardiac death (Q3925E)[10,11] and the other (E3848A) not yet known for relevance with cardiac pathology. We also measured directly the RyR2-mediated Ca^{2+}-release from the SR in mutant and wild type (WT) myocytes by infecting them with a genetically targeted SR probe (ER-GCaMP6)[17] and monitored simultaneously the cytosolic rise in calcium using Fura-2 probe.

The aberrancies in calcium signalling of the two mutations were similar. Both mutant lines derived cardiomyocytes had suppressed I_{Ca}- and caffeine-triggered Ca^{2+} releases despite no change or enhanced I_{Ca}. Unexpectedly, spontaneous, at times arrhythmic, Fura-2 monitored Ca^{2+} transients persisted in mutant cells, but such Fura-2 transients were unaccompanied by the SR calcium release signals, consistent with greatly suppressed Ca^{2+}-induced Ca^{2+} release (CICR), suggesting a shift (remodelling) of calcium signalling pathway to one dominated by influx of calcium through the channel and/or Ca^{2+} release from other cellular Ca^{2+} pools.

2. Methods

2.1 Maintenance of undifferentiated hiPSC lines

Human-induced pluripotent stem cells K3 line[18] was provided from Duncan lab at Medical University of South Carolina and used as the WT cell line as described in previous publications.[19,20] Undifferentiated hiPSCs were maintained in StemFlex medium (Gibco) on Vitronectin (Gibco) coated 60 mm culture dishes at 37°C with 5% CO_2. The culture medium was replaced every 2 days and hiPSCs were passaged with Accutase (Thermo Fisher) every 4–6 days. A total of 10 μM Y-27632

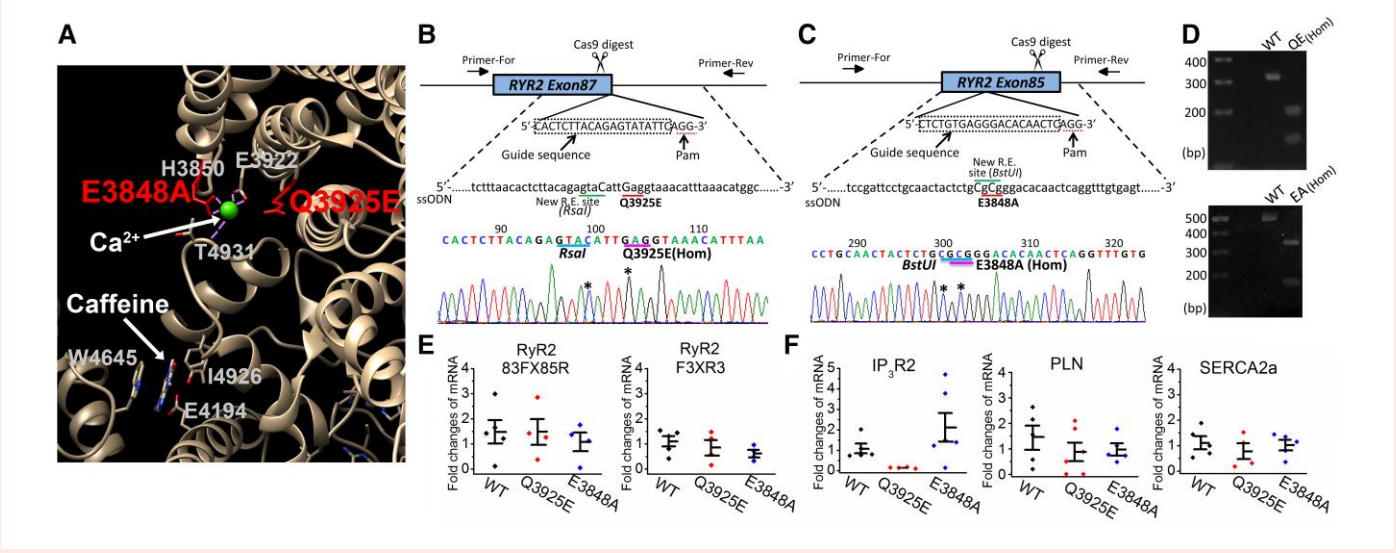

Figure 1 Introduction of Q3925E and E3848A mutation in *RYR2* gene of hiPSC. (*A*) The cartoon shows cryo-electron microgram of the Ca^{2+}- and caffeine-binding sites in RyR. Ca^{2+}-binding sites of skeletal RyR1 are formed essentially by five amino acid residues. Three corresponding RyR2 amino acid residues, E3848, E3922, and T4931 directly bind to Ca^{2+}, while H3850 and Q3925 are part of a secondary co-ordination sphere of Ca^{2+}. Structural data (PDB accession: 5TAL) are presented by Chimera program.[7] (*B*) Top, schematic of gene editing. Q3925E mutation (CAG to GAG) and a restriction enzyme site *RsaI* guide sequence was designed to target the Exon87 of *RYR2* in the hiPSCs. Bottom, sequencing of the mutated locus in the homozygote showed two mutations (*). One is RyR2 mutation and the other one does not change amino acid but creates restriction enzyme site. (*C*) Top, E3848A mutation (GAG to GCG) and the restriction enzyme site silent mutation were designed to target Exon85. Bottom, sequencing of the mutated locus in the homozygote showed two mutations (*). One is RyR2 mutation and the other one does not change amino acid but creates restriction enzyme site. (*D*) The gel images show PCR analysis of the Q3925E and E3848A homozygous mutants. The gene-edited regions of genomic DNA were amplified by PCR, and then digested by restriction enzyme. (*E*) Quantification of RyR2 transcription levels in WT and the two mutant hiPSC-CMs by quantitative RT–PCR. $n = 4$–5 differentiations. Data are shown as mean ± SEM. RyR2 transcription levels are not significantly difference between WT and mutant cells by one-way ANOVA. (*F*) Quantification of IP_3R2, PLN and SERCA2a transcription levels in WT and the two mutant hiPSC-CMs ($n = 4$–6) by quantitative RT–PCR. Data are shown as mean ± SEM. *$P < 0.05$ vs. WT by Student's *t*-test ($P = 0.018$), but not significant by one-way ANOVA.

ROCK inhibitor (Tocris) was added in the culture media for 24 h after each passage.

2.2 CRISPR/Cas9 genome editing in hiPSCs

CRISPR/Cas9 gene-editing technique was applied to introduce RyR2 mutation Q3925E into hiPSC genome as described before.[21] See supplementary materials online for detailed method.

2.3 Differentiation of hiPSCs into functional cardiomyocytes

CRISPR/Cas9 gene-edited Q3925E and E3848A hiPSCs were differentiated into cardiomyocytes by using the standard protocol (activate and block Wnt signalling) as described previously.[20]

2.4 Quantitative RT–PCR

Total RNAs of WT and mutant hiPSC-CMs were extracted with TRIzol LS reagent (Ambion, Life Technologies) and then purified by RNeasy kit (Qiagen). The cDNAs were synthesized from total RNAs by reverse transcription with Verso cDNA Synthesis Kit (Thermo Scientific). See supplementary method for detailed protocol and supplementary material online, Table *S1* for the primers.

2.5 Western blot

hiPSC-CMs monolayers were collected and washed three times with cold DPBS, then omogenized for 15 min in ice-cold RIPA buffer (Thermo Scientific) containing protease inhibitor cocktail (Thermo Scientific). Protein lysates were obtained after centrifugation at 12 000 *g* for 15 min at 4°C. BCA Assay Kit (Thermo Scientific) was used to measure the protein concentrations. WT and Q3925E mutant proteins (16 μg/lane) were separated on 4–15% precast polyacrylamide gels (Bio-Rad) and transferred overnight to polyvinylidene difluoride membranes. A total of 3% BSA was used to block the membranes at room temperature for 1 h followed by overnight incubation at 4°C with primary antibodies: anti-Ryanodine Receptor Monoclonal Antibody (C3–33) (1:1000, Thermo Scientific) and anti-GAPDH (D16H11) (1:1000, Cell Signaling Technology) as control.

The membranes were then incubated in the appropriate horseradish peroxidase-conjugated secondary antibody solution for 1 h at room temperature. Detection of bound antibody was performed using the SuperSignal West Femto Maximum Sensitivity Substrate (Thermo Scientific). All experiments were repeated four times ($n = 4$).

2.6 Measurements of ca^{2+} transients and sparks

hiPSC-CMs were dissociated using 10 × TrypLE™ Select enzyme (Gibco) and plated on vitronectin coated 25 mm glass coverslips and allowed to recover in culture medium for at least 3 days prior to imaging. Cells were incubated in 1 μM of Fluo-4 AM containing solution for 30 min and imaged using a multicolour total internal reflection fluorescence (TIRF) imaging system (Leica Microsystems, Buffalo Grove, IL).[22] An argon ion laser was used for excitation of Fluo-4 and ER-GCaMP6 at 488 nm and the fluorescence emission was measured at 502–548 nm. When using Fura-2 fluorescence, cells were excited at 405 nm and emitted fluorescence was measured at 420–470 nm. Ca^{2+} transients and sparks were recorded at 60–80 Hz with a depth of penetration of 110–150 nm to focus

primarily on the sub-sarcolemmal Ca^{2+} release. Sparks data were exported and analysed with Leica LAS X and a computerized algorithm described previously.[23]

2.7 Electrophysiology

Membrane currents of WT and mutant hiPSC-CMs were recorded at 30–32°C using the whole cell mode of patch clamp technique, employing a Dagan amplifier and pClamp software (Clampex 10.6). See supplementary materiala online for detailed method.

2.8 ER-GCaMP6 Ca^{2+} probe

ER-GCaMP6-150 cDNA plasmid[17] (#86918) was purchased from Addgene (Watertown, MA). Adenovirus carrying ER-GCaMP6-150 was produced by Vector Biosystems Inc. (Malvern, PA). Some 24–48 h after plating the hiPSC-CMs on 25 mm coverslips, the cells were infected by a solution containing ER-GCaMP6 adenovirus containing (MOI) of 300–500 virus particles per cell (vp/cell).[24] After 6–8 h, the virus medium was removed, and cells were supplemented with B27+ medium and kept in the incubator at 37°C and 5% CO_2 until their use between 48 and 72 h post-infection.

2.9 Immunostaining

WT and mutant cells from 2–5-months old were dissociated and plated onto matrigel-coated coverslips. Next day, cells were infected by a solution containing FKBP-GCaMP6 adenovirus containing (MOI) of 300–500 vp/cell. Three days after FKBP-GCaMP6 infection, cells were stained with anti-Myosin Light Chain 2 (MYL2) antibody (Abcam, Cat. No. ab79935). See supplementary materials online for detailed method.

2.10 Statistical analysis

Results are indicated as the means ± SEM. Comparative analysis was determined using one-way analysis of variance (ANOVA) followed by Tukey's test or Student's *t*-test. Significant differences are labelled with one ($*P < 0.05$) or two asterisks ($**P < 0.01$). Origin 8 (OriginLab) was used to obtain statistical values.

3. Results

3.1 Creation of Q3925E and E3848A mutant lines

Figure 1B shows the design to introduce Q3925E mutation (CAG to GAG) and the silent mutation (TAT to TAC) that create a *RsaI* restriction enzyme site, in *RYR2* Exon87. Genomic DNA of the gene-edited locus was amplified by PCR, followed by restriction digest by *RsaI*. The full-size PCR product was 319 bp. In the heterozygous (Het) mutant, the PCR products were partially digested by the enzyme (see Supplementary material online, *Figure S1B*). In the homozygous (Hom) mutant the PCR product was fully digested into two fragments of 193 and 126 bp (*Figure 1D*). The accuracy of gene edits and the resultant mutations were confirmed by sequencing of the PCR products. *Figure 1B* shows that the homozygous mutant carries the Q3925E mutation in both gene alleles, while in the heterozygote mutants only one gene allele carries the mutation, Supplementary material online, *Figure S1A*. *Figure 1C* similarly shows the glutamate to alanine mutation (GAG to GCG) and the silent mutation that creates *BstUI* restriction site in RyR2 Exon85. Sequencing result in *Figure 1C* shows that the E3848A mutation is expressed in both gene alleles of RyR2, where PCR product amplified from the mutation locus of genomic DNA was completely restriction digested by *BstUI* into 329 and 163 bp (*Figure 1D*). We also confirmed both Q3925E and E3848A RyR2 mutations by sequencing the RT–PCR products amplified from total RNA of the beating hiPSC-derived cardiomyocytes (data not shown). Our RT–PCR and sequencing results of two homozygous Q3925E mutant lines and one heterozygous mutant line showed one possible splice variant lacking the entire exon87, but E3848A mutants showed no splicing variant at the exon85/intron85-86 boundary. To eliminate possible off-targeting effects, we established two homozygous Q3925E and two E3848A lines. One of the E3848A clone is homozygous, and the other clone had one allele that carried the mutation, while the other allele had one nucleotide deletion resulting in reading frameshift, thereby expression of non-functional RyR2 subunit. We also analysed possible chances for off-targeting effects by two programs (http://crispor.tefor.net/ and https://cm.jefferson.edu/Off-Spotter/) but found relatively low chances for off-targeting mutations by CRISPR gene edit for both mutations (see Supplementary material online, *Table S2*).

3.2 Quantitative PCR and western blot analysis of RyR2 expression

Quantitative PCR and western blot were used to detect the mRNA and protein levels of RyR2 in WT and mutant hiPSC-CMs. Total RNA and protein levels were measured around Day 40 after the initiation of spontaneous beating. We used a pair of 83F and 85R primers amplifies RyR2 cDNA regardless of existence of a splicing variant lacking entire exon 87, whereas a pair of 87F and 88R does not amplify the cDNA from the splicing variant. Quantitative RT–PCR analyses showed that the expression level of RyR2 messenger RNA in Q3925E and E3848A mutant hiPSC-CMs were essentially the same as WT cells, *Figure 1E*. RyR2 protein levels as determined by western blot also showed no significant differences between WT and Q3925E mutant groups (see Supplementary material online, *Figure S1C*). We also tested the mRNA expression of other Ca^{2+} handling genes. Quantitative RT–PCR analyses of phospholamban (PLN) and SERCA2a mRNA in Q3925E and E3848A mutant hiPSC-CMs were comparable to WT, *Figure 1F*. The expression level of IP_3R2 messenger RNA in Q3925E was lower as compared to WT, *Figure 1F*. However, the threshold cycles (CT) values for IP_3R2 are 30–32 for WT, 29.5–33 for E3848A, and 33–35 for Q3925E, suggesting relatively poor expression of IP_3R2.

3.3 L-type Ca^{2+} current and CICR in Q3925E and E3848A homozygous mutant cardiomyocytes

To confirm that our WT and mutant cardiomyocytes were mostly of atrial/ventricular origins, we infected the cells with FKBP-GCaMP6[22] and then stained them with anti-Myosin Light Chain 2 antibody, Supplementary material online, *Figure S2*. Since MYL2 is specifically expressed in ventricular tissue,[25,26] the representative cell images shown in Supplementary material online, *Figure S2*, showing strong expression of MYL2 with sarcomeric pattern of FKBP, confirm that most of our cells were of ventricular origins.

L-type Ca^{2+} current and their triggered Ca^{2+} transients were measured in WT and mutant hiPSC-CMs dialyzed with pipette solutions containing 0.1 mM Fluo4 penta-potassium salt and 0.1 mM EGTA plus 0.3 mM Ca^{2+} using TIRF-imaged whole-cell voltage-clamped cells. Cardiomyocytes were either depolarized from −50 to 0 mV to activate I_{Ca} or repolarized from +100 to −50 mV that activated I_{Ca} tail currents triggering Ca^{2+} transients. Because I_{Ca} tail-current protocol deactivates the channel rapidly, this protocol minimized the contribution of transmembrane influx of Ca^{2+} through the channel to the global Ca^{2+} transients (*Figure 2A*). We consistently found larger rises of cytosolic calcium with depolarizing pulses to zero compared to repolarizing pulses that activate I_{Ca} fully but deactivate it rapidly at −50 mV, (*Figure 2B–E*). Peak I_{Ca} current densities in cardiomyocytes differentiated from two different homozygous Q3925E mutant lines were slightly larger than in WT cells, averaging: -9.99 ± 0.66 pA/pF ($n = 38$) in the first homozygous line (*Figure 2D*) and -11.45 ± 1.04 pA/pF ($n = 27$) in the second homozygous line (see Supplementary material online, *Figure S3D*) as compared to -8.57 ± 0.61 pA/pF in WT ($n = 45$). There was also consistent slowing in the kinetics of inactivation of I_{Ca} in mutant cells, *Figure 2F*, which contributes to enhanced transmembrane influx of calcium, see also *Figure 3B*.

In cardiomyocytes from two E3848A mutant lines peak I_{Ca} current densities were not significantly enhanced, (averaging about -8.46 ± 0.56, $n = 35$ and -9.70 ± 0.67, $n = 32$), but I_{Ca}-triggered Ca^{2+} transients were greatly suppressed in both Q3925E and E3848A homozygous lines, *Figure 2B–E*

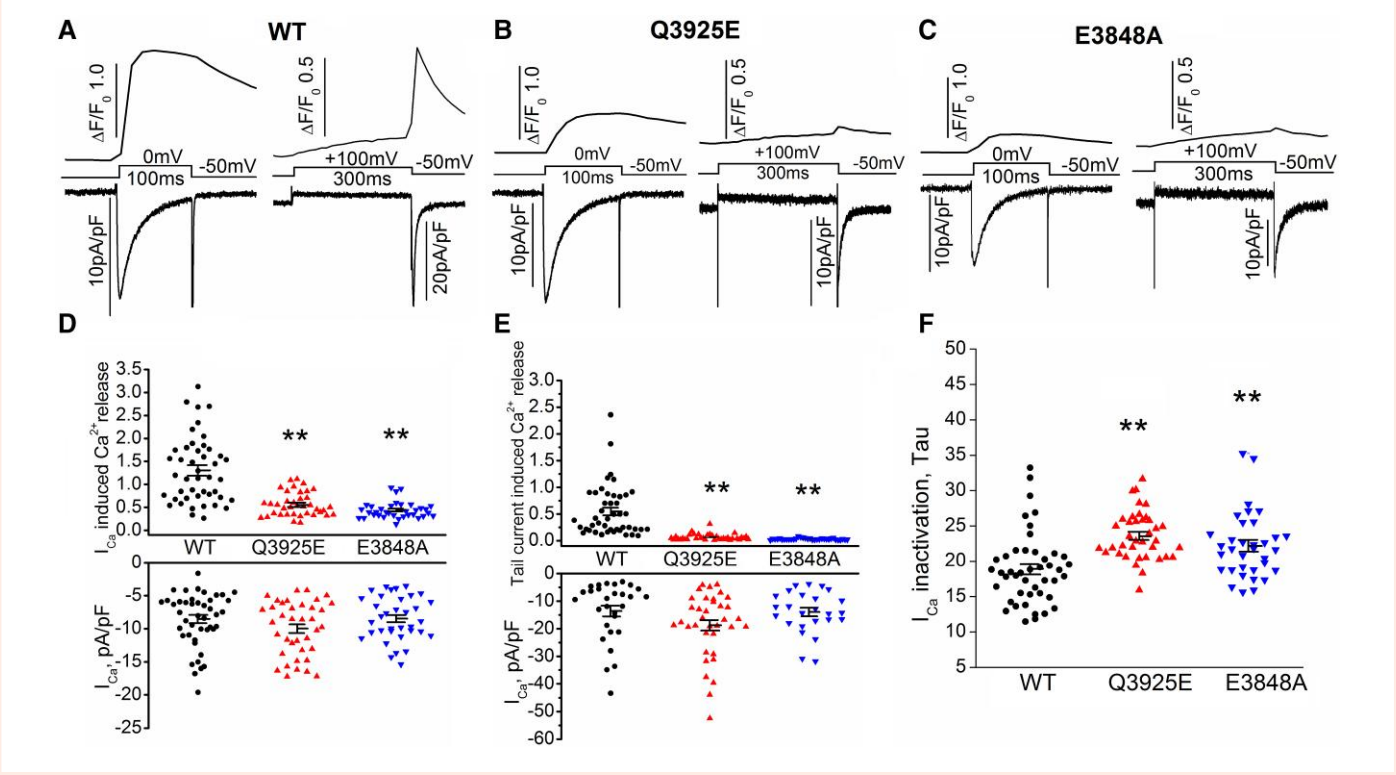

Figure 2 Simultaneous measurements of L-type Ca^{2+} currents and I_{Ca}-induced Ca^{2+} transients in whole cell patch clamped WT, Q3925E, and E3848A homozygous mutant hiPSC-CMs. (*A–C*) Representative traces of I_{Ca} currents and I_{Ca}-induced Ca^{2+} transients recorded at depolarizations to zero mV (left traces) and repolarization from +100 mV to −50 mV (right traces) in WT and mutant hiPSC-CMs. (*D*) Quantification of I_{Ca} density and I_{Ca}-triggered Ca^{2+} transients ($\Delta F/F_0$) in WT and mutant hiPSC-CMs. $n = 45$, 38, and 35 for WT, Q3925E, and E3848A, respectively. (*E*) I_{Ca} tail currents and tail currents triggered Ca^{2+} transients in WT and mutant hiPSC-CMs were quantified. Top, $n = 45$, 36, and 34 for WT, Q3925E, and E3848A. Bottom, $n = 29$, 36, and 25 for WT, Q3925E, and E3848A. (*F*) Quantification of time constants (in ms) of inactivation of I_{Ca} (Tau) in WT and mutant hiPSC-CMs. $n = 45$, 38, and 34 for WT, Q3925E, and E3848A. A total of 0.1 mM Fluo-4 salt was dialyzed through patch pipet. Data are shown as scatter dots with mean ± SEM. $^{**}P < 0.01$ vs. WT by one-way ANOVA followed by Tukey's test.

and Supplementary material online, *Figure S3B–E*. Heterozygous Q3925E mutant cardiomyocytes also had significantly suppressed I_{Ca}-induced Ca^{2+} release, Supplementary material online, *Figure S1D*. Quantitative comparison of I_{Ca}-triggered Ca^{2+} release in both heterozygous and homozygous lines of E3848A and Q3925E suggests that mutation of either residue of RyR2 Ca^{2+}-binding site, irrespective of their established association with cardiomyopathy, greatly impairs CICR.

3.4 Spontaneous focal calcium releases in Q3925E mutant cells

To test the effects of Ca^{2+}-binding site mutation on focal Ca^{2+} releases, we measured the morphology and the frequency of spontaneously igniting Ca^{2+} sparks in WT, Q3925E, and E3848A mutant cells. It should be noted that most mutant cells failed to show spontaneously igniting calcium sparks, consistent with greatly suppressed CICR shown in *Figure 2*. Nevertheless, we were able to measure spontaneously igniting Ca^{2+} sparks in 7 out of 100 Q3925E and 3 out of 100 E3848A cells and quantify their morphology and frequency. Supplementary material online, *Figure S4* shows that spontaneously triggered Ca^{2+} sparks were brief, less frequent, ignited rapidly, and decayed slowly in Q3925E hiPSC-CMs compared to WT cells. Sparks frequency was significantly suppressed in both Q3925E and E3848A, Supplementary material online, *Figure S4D*. The histogram of spark duration, measured at half-maximum amplitude, averaged 56.97 ± 1.77 ms in WT cells vs. 66.73 ± 5.6 ms in Q3925E-homozygote and 46.67 ± 4.85 ms in E3848A-homozygote, Supplementary material online, *Figure S4E*.

3.5 ER-GCaMP6 targeted SR probe signals in WT and mutant myocytes.

To quantify possible contribution of different sources of cellular calcium to I_{Ca}- or caffeine-triggered Ca^{2+} transients in mutant myocytes, whole cell clamped myocytes infected with genetically engineered ER/SR localized calcium probe (ER-GCaMP6), and dialyzed with Fura-2, were subjected to puffs of caffeine and step depolarizing pulses that activated I_{Ca}. *Figure 3A* and *C* show a large rise of cytosolic Ca^{2+} (Fura-2 signal) and significant decrease in simultaneously measured SR calcium content on activation of I_{Ca} or application of 5 mM caffeine in WT cells. In either Q3925E or E3848A mutant myocytes activation of a large I_{Ca} (*Figure 3A* and *B*), comparable to WT cells, though causing a significant rise in cytosolic Ca^{2+} (Fura-2 signal), failed to activate significant SR Ca^{2+} release signals. The significant rise in cytosolic calcium (Fura-2 signal), triggered by I_{Ca} in both Q3925E and E3848A mutant cells, results most likely from enhanced transmembrane influx of calcium through the channel as reflected in the measurements of integral of Ca^{2+} current, *Figure 3B*. Similarly, 5 mM caffeine that activated a large rise in Fura-2 signal, generating a large I_{NCX}, and SR calcium release signal (ER-GCaMP6 signal, *Figure 3C* and *D*) in WT cells, failed to trigger either significant Fura-2 signal and I_{NCX}, or activate an SR calcium release signal in mutant cells, consistent with mutation-induced suppression of CICR.

In a set of WT and mutant cells that were not spontaneously beating, trains of depolarizing pulses from −50 to 0 mVs were applied to activate I_{Ca}-triggered rise of cytosolic Ca^{2+} (Fura-2 signal) and the accompanying SR calcium release signals (ER-GCaMP6 signals). *Figure 4A* shows that application

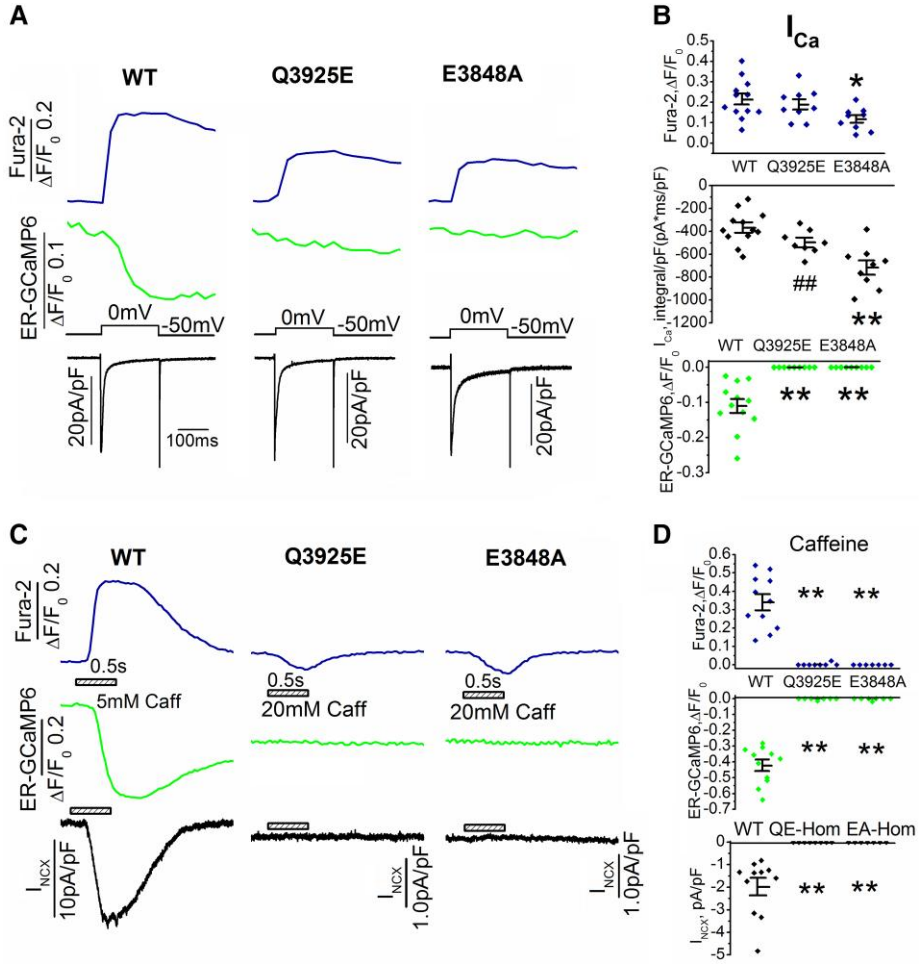

Figure 3 Simultaneous measurements of L-type Ca^{2+} currents, I_{Ca}-induced Ca^{2+} transients, and caffeine-induced Ca^{2+} by Fura-2 and ER-GCamP6 in whole cell patch clamped WT, Q3925E, and E3848A mutant hiPSC-CMs. (*A*) Representative traces of I_{Ca} currents (black), I_{Ca}-induced cytosolic Ca^{2+} transients (blue), and SR Ca^{2+} release (green) recorded at depolarizations to zero mV in WT and mutant hiPSC-CMs. (*B*) Quantification of I_{Ca} current integrals (black) and I_{Ca}-triggered Ca^{2+} release measured by Fura-2 (blue) and ER-GCaMP6 (green) in WT and mutant cells. $n = 12$, 9, and 9 for WT, Q3925E, and E3848A, respectively. (*C*) Representative traces of caffeine-induced cytosolic (blue) Ca^{2+} rise and SR (green) Ca^{2+} release and I_{NCX} (black) in WT and mutant cells. (*D*) Quantification of caffeine-triggered I_{NCX} and Ca^{2+} release measured by Fura-2 and ER-GCaMP6. $n = 11$, 8, and 7 for WT, Q3925E, and E3848A, respectively. $^{*}P < 0.05$ vs. WT, $^{**}P < 0.01$ vs. WT by one-way ANOVA followed by Tukey's test. $^{\#\#}P < 0.01$ vs. EA.

of train of depolarizing pulses followed by application of 5 mM caffeine triggered both transient increases in cytosolic calcium (Fura-2) and release of calcium from the SR (ER-GCaMP6 signal) in WT cells that activated also significant Na^{+}/Ca^{2+} exchange current, I_{NCX}. Similar trains of depolarizing pulses in either Q3925E or E3848A mutant cells, though activating I_{Ca}-triggered Fura-2 transients, failed to trigger either I_{Ca}- or caffeine-triggered ER-GCaMP6 signals (*Figure 4B–D*). The significant rise in the cytosolic calcium (Fura-2 signal) is likely to be caused by the larger (50–100%) and slower influx of transmembrane calcium in the mutant cells, *Figure 4D*. These finding suggest that E3848A and Q3925E mutant myocytes have significantly suppressed CICR and decreased caffeine sensitivity.

3.6 Spontaneous beating in intact WT and mutant cells

We were surprised to find that the beating frequencies of mutant cardiomyocytes monolayers in culture media were not significantly different than those of WT cells. In isolated cardiomyocytes, however, while WT cells maintained constant beating rates, the mutant cells had mostly arrhythmic and variable beating rates, with individual calcium transients having variable durations and amplitudes. *Figure 5* compares the spontaneously activating calcium transients measured with both the SR and cytosolic probes in one WT and two Q3925E and two E3848A mutant cells. Most unexpected was that both mutant cell lines continued to beat spontaneously and mostly arrhythmically activating Fura-2 signals, but failed to generate significant SR calcium release signals, *Figure 5B* and *C*, consistent with their greatly suppressed CICR (*Figure 2*).

To identify the source of cytosolic Ca^{2+} signal that persists in absence of ER Ca^{2+} release signal, the cells were exposure to 200 μM $CdCl_2$, 1 μM nifedipine or 10 μM cyclopiazonic acid (CPA), SERCA inhibitor.[27,28] Cd^{2+} and nifedipine consistently blocked the spontaneous beating in both WT and mutant cells, while CPA suppressed only the spontaneous ER Ca^{2+} release in WT myocytes without significantly affecting the cytosolic spontaneously triggered Ca^{2+} transients in both WT and mutant cells, *Figure 6*.

3.7 Ca^{2+} content of SR in WT and Q3925E or E3848A mutant myocytes

Since I_{Ca}-triggered Ca^{2+} releases were significantly suppressed in both mutant lines, we tested whether the suppression was caused by a decrease in SR calcium content, using 5 and 20 mM caffeine or 1 mM 4-CmC (another

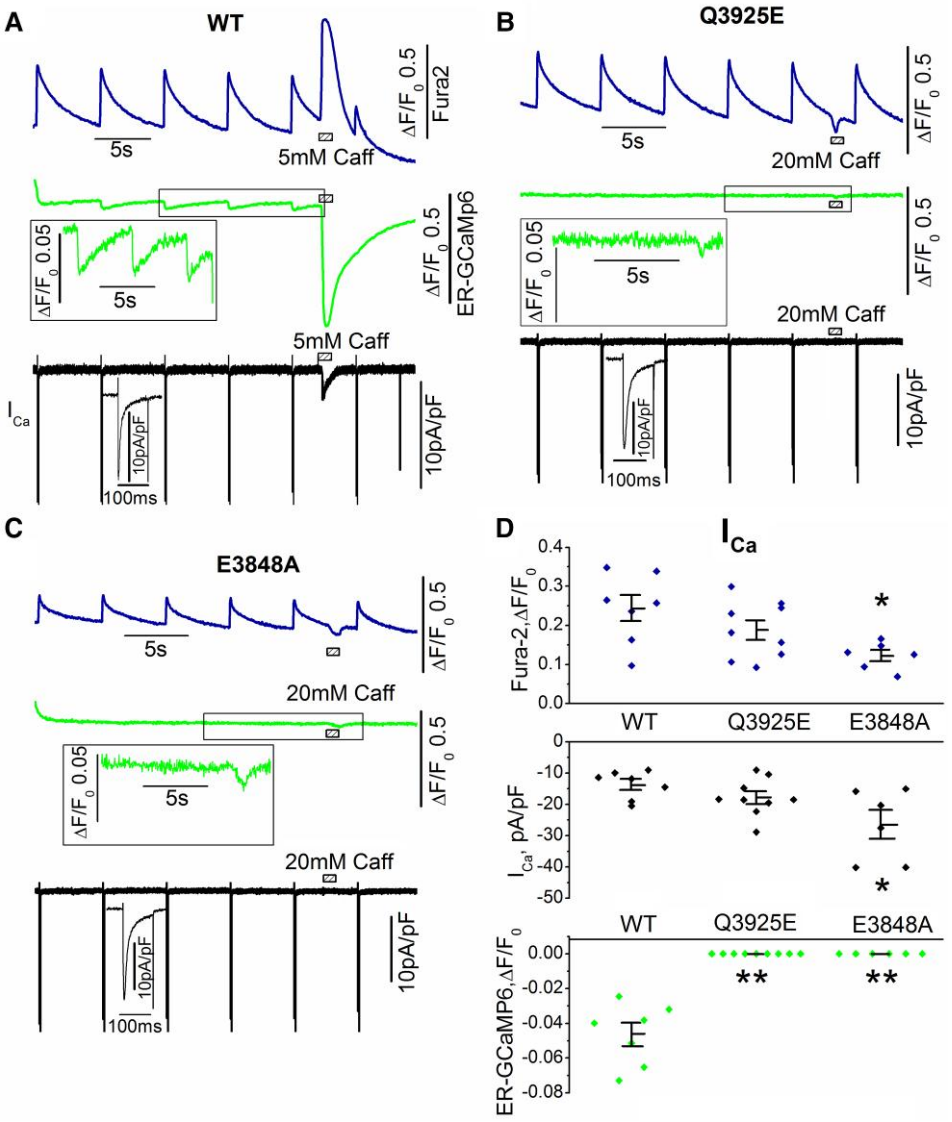

Figure 4 Simultaneous measurement of SR and cytosolic Ca^{2+} triggered by I_{Ca} train and caffeine in patch clamped WT, Q3925E, and E3848A cells. (*A–C*) The time course of cellular Ca^{2+} transients (blue), SR Ca^{2+} release (green), and I_{Ca} and caffeine stimulated I_{NCX} traces (black) in WT and mutant cells. Cells were stimulated by depolarization at 0.2 Hz (pulse train) and then triggered by caffeine for 1 s. Enlarged green traces show SR Ca^{2+} releases. Enlarged black traces show the I_{Ca} trace from the pulse train. (*D*) Quantization of I_{Ca} density and I_{Ca}-triggered Ca^{2+} releases measured by Fura-2 and ER-GCaMP6 in WT and mutant cells. $n = 7$, 9, and 6 for WT, Q3925E, and E3848A, respectively. *$P < 0.05$ vs. WT, **$P < 0.01$ vs. WT by one-way ANOVA followed by Tukey's test.

RyR2 agonist). In this set of experiments, a large number of single *intact* WT and mutant cells were subjected to the two drugs. In WT cardiomyocytes 5 or 20 mM caffeine produced equivalent, about two-fold, increase in cytosolic calcium, *Figure* 7*A*, *D*, and *E*, ($n = 64$ cells). In sharp contrast, in mutant cells 5 mM caffeine-triggered calcium release was mostly smaller in E3848A cells and was present in only ~ 20% of cells (25/128 of Q3925E mutant, and 9/43 of E3848A mutant) as compared to ~70% of cells with 20 mM caffeine (compare *Figure* 7*D* and *E*). Even though 95% of E3848A cells responded to 20 mM caffeine, the amplitudes of such Ca^{2+} transients were significantly smaller than those of control cells. The 20 mM caffeine-triggered rise in cytosolic Ca^{2+} in both mutants were also greatly delayed, had significantly slower rate of rise, and developed often at the end of 1 s long caffeine pulses, and their rate of rise were greatly slowed as compared to WT cardiomyocytes (time-to-peak Ca^{2+} rise increasing from 0.25 to 1.0 s, *Figure* 7*B*, *C*, and *F*).

Application of 1.0 mM 4-CmC in WT cells similarly triggered about two-fold increase in cytosolic calcium (compare *Figure* 7*H*, *D*, and *E*). In mutant cells, however, even though 4-CmC triggered somewhat smaller calcium transients, there was no significant difference in the time to peak of Ca^{2+} release as compared to WT cells, *Figure* 7*H*. 4-CmC induced Ca^{2+} release in E3848A mutant were similarly smaller compared to WT or Q3925E mutant, *Figure* 7*H*. Thus, the cumulative data from intact cells, using 4-CmC and caffeine, suggest that the loss of 5 mM caffeine release signal in mutant cells was not caused by depleted SR pools, but by decreased sensitivity of RyR2 to caffeine. The increased percentage of mutant cells triggering Ca^{2+} release at higher caffeine concentrations but with suppressed and delayed kinetics may suggest that other pools of cellular calcium contribute to the 20 mM caffeine response. Cardiomyocytes derived from the second clones of Q3925E and E3848A mutants showed similar responses to 5 and 20 mM caffeine and 4-CmC (see Supplementary material online,

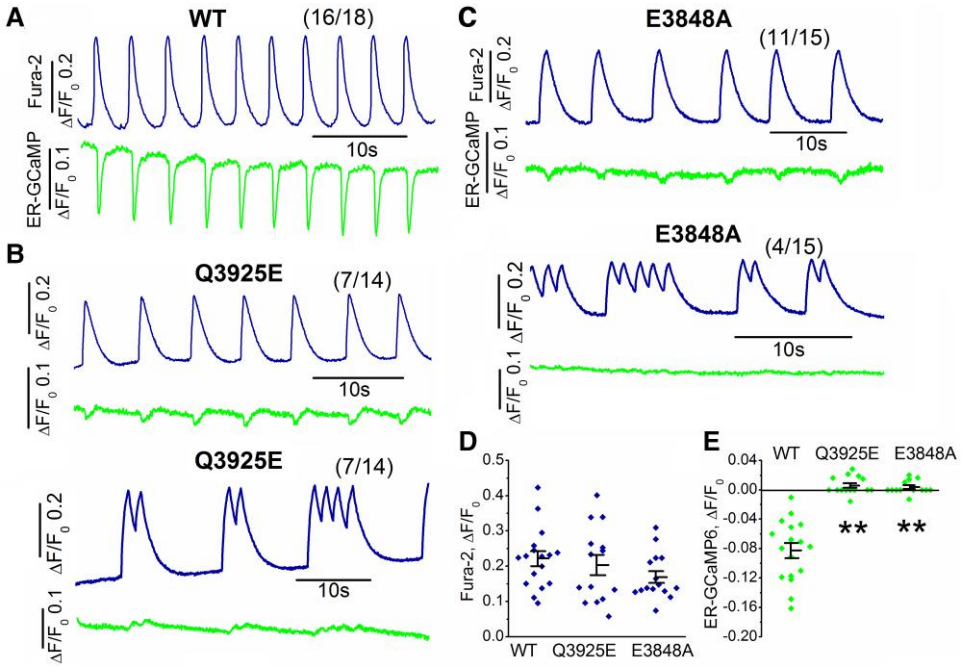

Figure 5 Spontaneous SR Ca^{2+} release and cytosolic Ca^{2+} transients measured by ER-GCaMP6 and Fura-2 in intact WT, Q3925E, and E3848A cells. (*A–C*) Representative traces of spontaneous beating measured simultaneously from cytosolic Ca^{2+} transients (blue) and SR Ca^{2+} release (green) in WT cell, regular beating and arrhythmogenic Q3925E and E3848A cells. Seven out of 14 Q3925E cells and 4 out of 15 E3848A cells show irregular Ca^{2+} transients. (*D–E*), Quantification of Ca^{2+} transients and SR Ca^{2+} release measured by Fura-2 and ER-GCaMP6 in WT, Q3925E, and E3848A cells. $n = 17$, 14, and 15 for WT, Q3925E, and E3848A, respectively. $^{**}P < 0.01$ vs. WT by ANOVA with Tukey.

Figure S5). The finding that 4-CmC induced Ca^{2+} release were consistently smaller in mutant cells suggests that the SR calcium content maybe also suppressed.

In another set of experiments in intact cells, WT and mutant cells were infected with ER-GCaMP6 and incubated with Fura-2 AM. Supplementary material online, *Figure S6* show that while both 5 mM 4-CmC and 5 mM caffeine-triggered large rise of cytosolic Ca^{2+} (Fura-2 signal) and significant decrease in simultaneously measured SR calcium content (ER-GCaMP6 signal) in WT myocytes, in mutant cells 5 mM 4-CmC triggered significantly smaller Ca^{2+} transients and ER Ca^{2+} release, compare Supplementary material online, *Figure S6B and D*. Note that in both mutant lines, the 20 mM caffeine-triggered responses were slow and delayed, consistent with *Figure 7*. Note also that the accompanying ER Ca^{2+} release triggered by 20 mM caffeine in the mutant cells were significantly impaired, consistent with the spontaneous beating data in *Figures 5* and *6*.

3.8 Pool of calcium activated by 20 mM caffeine in mutant cardiomyocytes

To identify the pool of calcium activated by 20 mM caffeine and determine the contribution of SR to it, an inhibitor of SERCA2a, CPA, was used to suppress SR calcium content. We found that while 10 μM CPA effectively suppressed both 5 and 20 mM caffeine-triggered ER and Fura-2 Ca^{2+} release signals in WT cells, Supplementary material online, *Figure S7A*, in mutant cells the slowly activating and delayed 20 mM caffeine-triggered cytosolic Ca^{2+} rise was not significantly affected by CPA, Supplementary material online, *Figure S7B and C*, suggesting that 20 mM caffeine-triggered cytosolic Ca^{2+} rise in the mutant cells did not directly originate from the SR. Although CPA seems to suppress significantly the 20 mM caffeine-triggered response in Q3925E cells (see Supplementary material online, *Figure S7B'*), the suppressive effect seemed to depend on the magnitude of ER signal generated by application of caffeine, such that in cells where caffeine activated a large ER signal, CPA was very effective in suppressing the caffeine-triggered calcium release. On the other hand, in cells that failed to activate an ER signal or where ER release signal was small, CPA failed to suppress the caffeine signal, suggesting multiple cellular pools contributing to the 20 mM caffeine transients.

To further probe the identity of the cellular calcium pools that contributes to the 20 mM caffeine response in mutant cells, we used a host of pharmacological agents that are known non-specifically[29–34] to suppress the various cellular calcium transporting pathways that include TRP channels, IP_3 receptors, store operated Ca^{2+} release, hemi-channels, and mitochondria. Supplementary material online, *Figure S8* shows that although 50 μM 2-APB and 10 μM ruthenium red significantly suppressed the 20 mM caffeine responses in a subset of cells, the degree of drug-induced suppression varied greatly among the mutant cells. In some of E3848A mutant cardiomyocytes, application of 20 mM caffeine often produced two phases of cytosolic rise of calcium, Supplementary material online, *Figure S8C and F*. The slow first component was generally suppressed by zero calcium solutions (see Supplementary material online, *Figure S9A*) suggesting transmembrane influx of calcium, on application of high concentrations of caffeine, possibly through activation of TRP- or hemi-channels. Even though the reported IC_{50} for 2-APB suppression of TRPM2 and TRPC5 ranges between 1 and 20 μM,[30,31] in some of our cells even 50 μM 2-APB failed to suppress the release of calcium. The cellular variability in suppressive effects of 2-APB, ruthenium red, or mitochondrial uncoupler FCCP on the 20 mM caffeine responses, Supplementary material online, *Figures S8 and S9B*, suggests that different calcium pathways may have been activated in different cells to compensate for the suppressed CICR. Thus, the variability in effectiveness of various drugs may reflect the diversity in expression of different calcium pools (remodelling) to compensate for loss of CICR and activation of SR pools.

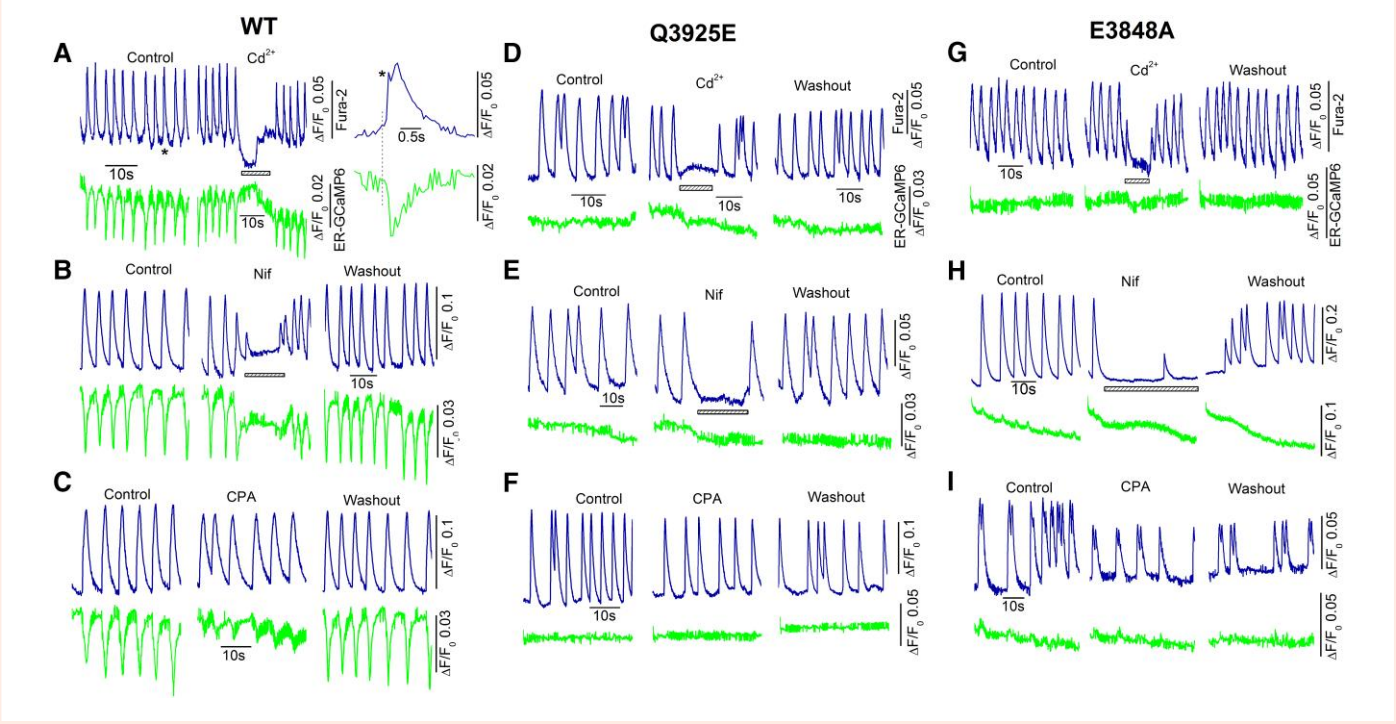

Figure 6 Effect of $CdCl_2$, nifedipine, and CPA on spontaneous beating WT and mutant hiPSC-CMs measured by ER-GCaMP6 (green) and Fura-2 (blue). (*A*) Representative traces of spontaneous beating before and after exposure to 200 μM $CdCl_2$ in WT cells. Right panel shows enlarged Fura-2 and ER-GCaMP6 traces indicated by asterisk (*). $n = 8$. (*B*) Representative traces of spontaneous beating before and after exposure to 1 μM nifedipine in WT cells. $n = 6$. (*C*) Representative traces of spontaneous beating before and after exposure to 10 μM CPA in WT cells. $n = 6$ (*D–F*) Representative traces of spontaneous beating before and after exposure to 200 μM $CdCl_2$, nifedipine, and CPA in Q3925E cells. $n = 8$, 8, and 6 for $CdCl_2$, nifedipine, and CPA, respectively. (*G–I*) Representative traces of spontaneous beating before and after exposure to 200 μM cadmium, nifedipine, and CPA in E3848A cells. $n = 9$, 6, and 6 for Cd^{2+}, nifedipine, and CPA, respectively.

3.9 Heterozygous RyR2 mutations

Since heterozygous mutations are more likely to represent the pathology encountered in human patients, we also examined the calcium signalling aberrancies that were expressed in heterozygous myocytes. Supplementary material online, *Figure S1D* shows that I_{Ca}-induced Ca^{2+} release was also significantly suppressed in the heterozygous Q3925E mutants, consistent with the findings in homozygous mutants. Heterozygous mutations, however, seem to retain their sensitivity to 5 mM caffeine, and the released Ca^{2+} was even larger than WT (see Supplementary material online, *Figure S1E*). In heterozygous Q3925E cells, RyR2s are most likely expressed in multiple different heterotetramers (six possible formations) that include the WT homotetramer. Assuming a random distribution, WT homotetramer is one out of 16 tetramers, and the heterotetramer with one Q3925E subunit is four out of 16. Thus, depending on the proportions of mutants expressed in RyR2 heterotetramers, the protein would variably respond to Ca^{2+} and caffeine, making Ca^{2+} signalling aberrancies less severe as compared to the homozygous cells. Our data show that one gene allele mutation is not sufficient to fully disable caffeine-triggered calcium release and suggests that homozygous mutation clones may better represent the pathology of the mutation.

4. Discussion

This is the first study that compares the EC-coupling consequences of mutating two of five residues of RyR2 Ca^{2+}-binding site in human cardiomyocytes, one of which, Q3925E, is reported to associate with sudden death. Although there is insufficient evidence for functional correlation of E3848A mutation to CPVT or other forms of arrhythmias, one variant of E3848 has been reported in ClinVar (E3848K mutation, accession: VCV000404231.16, https://www.ncbi.nlm.nih.gov/clinvar/). We predict that this E3848K mutation will also impair CICR and perhaps produce an even more severe clinical phenotype than E3848A mutation, as lysine's positive charge will greatly reduce the Ca^{2+} affinity of the site as compared to alanine.

We used CRISPR/Cas9 gene editing to introduce point mutations in stem cell derived human cardiomyocytes and infected the cells with an SR-targeted calcium-sensitive fluorescent probe, ER-GCaMP6, to directly measure the contribution of mutant RyR2 to cytosolic calcium levels measured with Fura-2 probe. It is clear that both Ca^{2+}-binding site mutations, irrespective of their association with cardiac pathology, disable CICR by suppressing I_{Ca}-triggered Ca^{2+} release, despite significant enhancement of calcium influx through the L-type calcium channels. The enhancement of calcium influx and variable pharmacological sensitivity of mutant cells to IP_3R and hemi-channel blockers, when calcium is released by high concentrations of caffeine, points to possible remodelling of calcium signalling pathway in response to disabling CICR. Since hiPSC-CMs, unlike the generally used HEK293 cells recombinant RyR2 platform,[9,12] express all the calcium signalling pathways of adult and neonatal mammalian cardiomyocytes,[16,35] it is likely that mutations that disable CICR function, may activate other dormant calcium signalling pathways of cardiomyocytes that would allow the mutant myocytes to survive and continue beating.

4.1 Q3925E mutation lack the entire exon87

Our RT–PCR experiments indicate that Q3925E mutation in *RYR2* exon87 most likely causes alternative splicing, consistent with the annotation by Ensembl Genome Browser (www.ensembl.org). We found two different RT–PCR products for the homozygous Q3925E mutant: one carrying

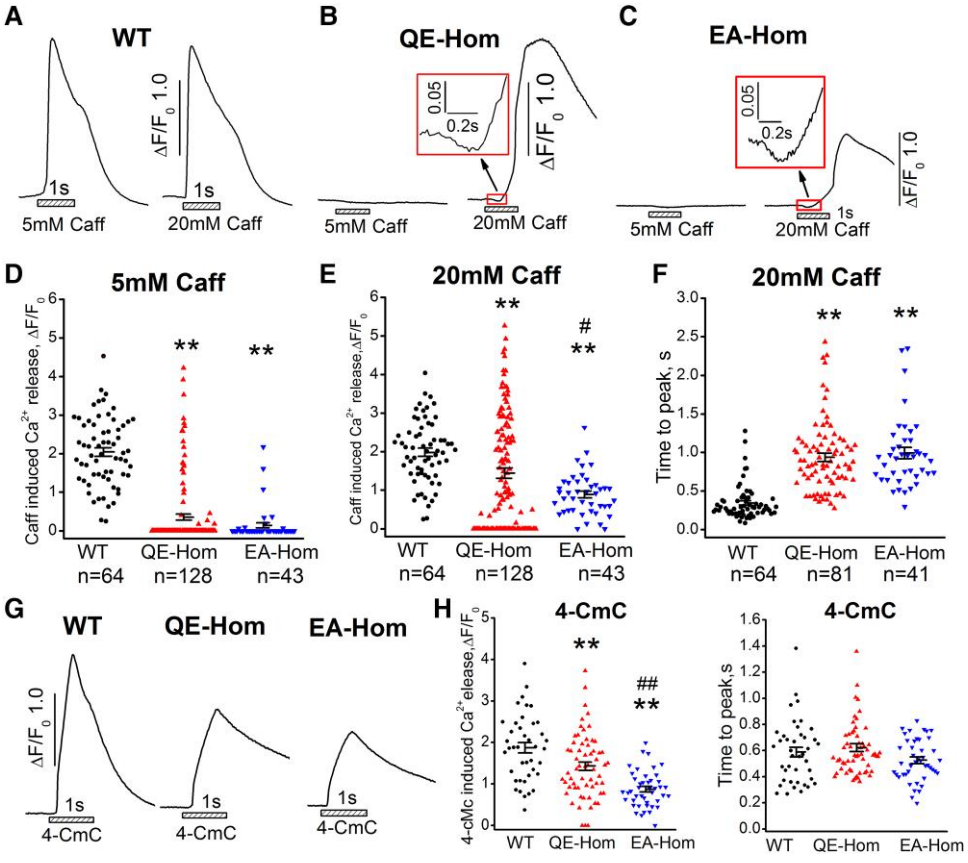

Figure 7 Caffeine and 4-CMC induced Ca^{2+} release in intact WT, Q3925E, and E3848A homozygous hiPSC-CMs. (*A–C*) Representative traces of 5 mM (left) and 20 mM caffeine (right)-triggered Ca^{2+} releases in WT and mutant hiPSC-CMs. (*D–E*) Quantification of the amplitude of 5 and 20 mM caffeine-induced Ca^{2+} releases was measured in Fluo-4 AM incubated WT, Q3925E, and E3848A mutant cells. $n = 64$, 128, and 43 for WT, Q3925E, and E3848A, respectively. (*F*) Time to peak of 20 mM caffeine-induced Ca^{2+} release in WT and mutant cells. $n = 64$, 81, and 41 for WT, Q3925E, and E3848A. (*G*) Representative traces of 1 mM 4-CmC triggered Ca^{2+} release in WT, Q3925E, and E3848A mutant cells. (*H*) Quantification of the amplitude and time to peak of 4-CmC induced Ca^{2+} releases in WT and mutant cells. Left panel, $n = 41$, 62, and 44 for WT, Q3925E, and E3848A. Right panel, $n = 41$, 59, and 44 for WT, Q3925E, and E3848A. Data are shown as mean ± SEM. $^{**}P < 0.01$ vs. WT, $^{\#\#}P < 0.01$ vs. QE by ANOVA with Tukey.

the desired Q3925E point mutation and the other lacking the entire sequence encoded by exon87 including Q3925. Since this deletion did not cause reading frameshifts, the homozygous mutant myocytes most likely express two different RyR2 subunits. It is not yet clear whether the subunit with the deleted exon87 can form a functional Ca^{2+} release channel, and whether these two subunit fragments (one with a single point mutation and the other with a large deletion segment) could form the RyR2 hetero tetramers. *In vitro* characterization of the recombinant protein carrying the deletion mutant might help resolve this issue. Although the recombinant Q3925E-RyR2 and the corresponding Q3970E-RyR1 have been reported to exhibit loss-of-function phenotype in the heterologous HEK293 cell platform,[12,14] consistent with our observation in human cardiomyocytes, the cardiomyocyte platform exhibiting the genetic remodelling and alternation of RNA splicing, may mimic better the complicated human patient pathology.

4.2 Possible interaction between Ca^{2+}- and caffeine-binding sites

Our data show that homozygous mutations of either Ca^{2+}-binding site residue suppressed both I_{Ca}- and caffeine-triggered calcium release. Although mutations in RyR2 Ca^{2+}-binding residues, irrespective of their association with cardiomyopathy, were expected to suppress I_{Ca}-induced Ca^{2+} release in heart cells, the suppression of caffeine-triggered release was somewhat unexpected. In this respect, while 5 and 20 mM caffeine were variably effective in triggering Ca^{2+} release in only ~20% to ~70% of intact and calcium-unbuffered homozygous Q3925E and E3848A myocytes, in whole-cell patched and calcium-buffered cells (0.1 mM EGTA plus 0.3 mM Ca^{2+}) caffeine-triggered calcium release was absent even though 5 mM 4-CmC (another RyR-agonist) continued to release calcium, ruling out that the SR stores were greatly compromised. The finding that the 20 mM caffeine-triggered responses had delayed onset, slower rate of development, were unaccompanied by ER-GCaMP6 Ca^{2+}-release signals, and were variably suppressed by non-specific IP_3R and TRP channel inhibitors, mitochondrial uncouplers, and hemi-channel blockers in mutant cells may suggest that at higher concentrations caffeine activates other cellular Ca^{2+} pools that are developed as a consequence of their suppressed CICR pathway.

The proximity of Ca^{2+}- and caffeine-binding site residues (*Figure 1A*) may underlie the functional interaction between I_{Ca}- and caffeine-triggered calcium release. The near-atomic resolution RyR structure suggests that the putative caffeine- and ATP-binding site residues are in the proximity of the Ca^{2+}-binding site residues, all interconnected through the carboxyl-terminal domain.[9] Murayama *et al.*[8] suggested that the caffeine-binding site may negatively regulate the Ca^{2+} sensitivity through interactions between tryptophan on the S2S3 and isoleucine on the CTD, providing a

mechanism for interaction of the two sites. Even though we confirmed in human cardiomyocytes that Ca^{2+}-binding site mutants have suppressed caffeine-induced Ca^{2+} release, it remains somewhat puzzling how changes in calcium sensitivity would result in the 20 mM caffeine-triggered slow and delayed responses, absence of ER-GCaMP6 SR-release signal, and calcium releases that are sensitive to blockers of IP_3R and hemi-channels. Alternatively, we suggest that significant cellular remodelling of calcium signalling pathways maybe taking place in the mutant cardiomyocytes with compromised CICR as to help maintain cellular contractility and survival.

4.3 Loss-of-function RyR2 mutations and CPVT

It is generally thought that RyR2 gain of function CPVT1 mutations are triggered by stress-induced catecholamine release that activate aberrant Ca^{2+} releases in the form of Ca^{2+} sparks, Ca^{2+} waves, or Ca^{2+} oscillations that lead to lethal arrhythmias and sudden cardiac death.[19,20,36,37] There are, however, reports that sudden cardiac death can also be triggered in individuals who have loss-of-function RyR2 mutations.[12,38,39] Such mutations have been recently classified as Ca^{2+} release deficiency syndrome to distinguish them from CPVT1.[38] Unfortunately, there has been only one case report on Q3925E mutation from post-mortem unexplained sudden death based on genetic testing but no exercise stress-induced tests.[10,11]

4.4 Physiological and pharmacological variabilities in hiPSC-CMs carrying mutations in calcium-binding residues of RyR2

Human stem cell derived cardiomyocytes are potentially an ideal platform to critically analyse the functional consequences of ion channel mutations on cellular levels as these cells are not only of human and cardiac origins with cardiac-specific calcium signalling pathways but are also conducive to gene editing using CRISPR/Cas9 technology. Nevertheless, it should be point out that hiPSC-CMs are developing cells and as such are likely to have subcellular organelles with undefined functions. Therefore, multifaceted experimental approaches must be undertaken to assure that these cells have at least the functional phenotype of adult cardiomyocytes. For instance, in evaluating cardiac calcium signalling, it is critical to analyse not only whether cells are spontaneously beating and generating cellular calcium transients, but also directly quantify the release of Ca^{2+} from SR vs. that measured in the cytosol. The efficiency of I_{Ca}-triggered calcium release (CICR gain), and its modulation by drugs and ionic interventions under precise electrophysiological and imaging conditions must be also quantified.[15,16] In the set of experiments reported here we used control cells that were 2–3 months old, expressed robust I_{Ca} density (~8 pA/pF) with bell-shaped voltage dependence to their Ca^{2+} transients, had large and rapid repolarization-triggered Ca^{2+} transients accompanying I_{Ca} tail currents, had high expression of IK1 and very low expression of I_f, generated calcium sparks and robust SR calcium release signals (ER-GCaMP6), and immunostaining suggested ventricular origins. It was somewhat surprising that mutant cells with defective RyR2 gene and suppressed I_{Ca}-gated Ca^{2+} release (disabled CICR), continued to beat spontaneously at rates equivalent to WT cells in monolayer cultures, or even in some isolated cells. Since electrophysiological and calcium imaging data clearly showed suppressed I_{Ca}-gated RyR2 pathway, it is likely that other dormant cardiac calcium signalling mechanisms are activated to maintain cellular viability and its function. Such remodelling may be in part responsible for the unexpected pharmacological cell-to-cell variability in sensitivity of mutant myocytes to drugs affecting other calcium transport pathways (see Supplementary material online, *Figures S8* and *S9*).

In WT hiPSC-CMs, our findings support a scheme where calcium channels provide the influx of calcium that activates the SR to release its calcium that activates first uptake of calcium by mitochondria followed then by release of calcium from mitochondria that contributes to slow relaxing phase kinetics of hiPSC-CMs calcium transients. In mutant CICR-disabled cells, where SR release triggered by I_{Ca} is suppressed, the enhanced influx of calcium may underlie directly mediate the calcium transients or activate the uptake and release of calcium from mitochondria or other ER calcium pools, and thus support spontaneous beating. The contribution of these pathways may vary with maturity of the myocytes and effectiveness of RyR2 mutation in disabling CICR.

4.5 Spontaneous beating in WT and mutant myocytes

The mechanisms responsible for spontaneous beating of hiPSC-CMs, has been subject significant scientific discourse and controversy. In a comprehensive study published recently by Chuck Murry's group[26] concluded that spontaneous beating results from multiple molecular mechanism. To obtain quiescent hESC-CMs they had to knock off multiple channels and transporters and over expressed others. In our cardiomyocytes, only L-type calcium channel blockers were consistently effective in suppressing spontaneous beating in WT or mutant myocytes. The spontaneous beating of the adult rat ventricular cells kept in culture media for 1–2 weeks was attributed to cells becoming flat and developing multiple protruding processes, where surface to volume ratio increases making the focal RyR2 release of calcium more effective in activating NCX to depolarize the cells and activate I_{Ca} to generate spontaneous activity.[40]

In CICR-suppressed but spontaneously beating mutant myocytes, although we have data supporting enhanced influx of calcium through the L-type or TRP channels and find variable sensitivity in suppressing the 20 mM caffeine-triggered transients by non-specific IP_3R or TRP channel blockers, we cannot rule out calcium release from nuclear envelop or other RyR1-gated pools. High concentrations of caffeine have been reported to activate large-conductance (200ps) hemi-channels in adult ventricular myocytes[34,41] and neonatal rat cardiomyocytes (data not shown) that can transport calcium and sodium that are blocked by ruthenium red.[34] Activation of large number of hemi-channels by high concentrations of caffeine may underlie the slow rise of cytosolic calcium on application industrial strength caffeine. Non-selective blockers such as 2-APB may also have suppressive effect on caffeine-activate hemi-channels resolving the conundrum of suppression of 20 mM caffeine-triggered calcium transients by IP_3R blockers.

Supplementary material

Supplementary material is available at *Cardiovascular Research* online.

Authors' contributions

Y.X. created all the mutant cell lines and did all the molecular biology experiments. X.-h.Z. did all the electrophysiology and Ca^{2+} imaging experiments. N.Y. designed the CRISPR/Cas9 mutations. M.M. designed and supervised the whole project.

Conflict of interest: None declared.

Funding

This work was supported by National Institutes of Health 1R01HL153504-01A1 to M.M., Jennifer Friedman Hillis Foundation, and the SC Blue Cross and Blue shield foundation.

Data availability

The data underlying this article will be shared on reasonable request to the corresponding author.

References

1. Pessah IN, Waterhouse AL, Casida JE. The calcium-ryanodine receptor complex of skeletal and cardiac muscle. *Biochem Biophys Res Commun* 1985;**128**:449–456.
2. Lai FA, Erickson H, Block BA, Meissner G. Evidence for a junctional feet-ryanodine receptor complex from sarcoplasmic reticulum. *Biochem Biophysical Res Commun* 1987;**143**:704–709.

3. Lai FA, Anderson K, Rousseau E, Liu QY, Meissner G. Evidence for a Ca^{2+} channel within the ryanodine receptor complex from cardiac sarcoplasmic reticulum. *Biochem Biophys Res Communications* 1988;**151**:441–449.
4. Kushnir A, Marks AR. The ryanodine receptor in cardiac physiology and disease. *Adv Pharmacol* 2010;**59**:1–30.
5. des Georges A, Clarke OB, Zalk R, Yuan Q, Condon KJ, Grassucci RA, Hendrickson WA, Marks AR, Frank J. Structural basis for gating and activation of RyR1. *Cell* 2016;**167**: 145–157 e117.
6. Gong D, Chi X, Wei J, Zhou G, Huang G, Zhang L, Wang R, Lei J, Chen SRW, Yan N. Modulation of cardiac ryanodine receptor 2 by calmodulin. *Nature* 2019;**572**:347–351.
7. Pettersen EF, Goddard TD, Huang CC, Couch GS, Greenblatt DM, Meng EC, Ferrin TE. UCSF Chimera—a visualization system for exploratory research and analysis. *J Comput Chem* 2004;**25**:1605–1612.
8. Murayama T, Ogawa H, Kurebayashi N, Ohno S, Horie M, Sakurai T. A tryptophan residue in the caffeine-binding site of the ryanodine receptor regulates Ca^{2+} sensitivity. *Commun Biol* 2018;**1**:98.
9. Guo W, Sun B, Estillore JP, Wang R, Chen SRW. The central domain of cardiac ryanodine receptor governs channel activation, regulation, and stability. *J Biol Chem* 2020;**295**: 15622–15635.
10. Medeiros-Domingo A, Bhuiyan ZA, Tester DJ, Hofman N, Bikker H, van Tintelen JP, Mannens MM, Wilde AA, Ackerman MJ. The RYR2-encoded ryanodine receptor/calcium release channel in patients diagnosed previously with either catecholaminergic polymorphic ventricular tachycardia or genotype negative, exercise-induced long QT syndrome: a comprehensive open reading frame mutational analysis. *J Am Coll Cardiol* 2009;**54**:2065–2074.
11. Tester DJ, Medeiros-Domingo A, Will ML, Haglund CM, Ackerman MJ. Cardiac channel molecular autopsy: insights from 173 consecutive cases of autopsy-negative sudden unexplained death referred for postmortem genetic testing. *Mayo Clinic Proceed* 2012;**87**:524–539.
12. Li Y, Wei J, Guo W, Sun B, Estillore JP, Wang R, Yoruk A, Roston TM, Sanatani S, Wilde AAM, Gollob MH, Roberts JD, Tseng ZH, Jensen HK, Chen SRW. Human RyR2 (ryanodine receptor 2) loss-of-function mutations: clinical phenotypes and in vitro characterization. *Circ Arrhythmia Electrophysiol* 2021;**14**:e010013.
13. Xu L, Chirasani VR, Carter JS, Pasek DA, Dokholyan NV, Yamaguchi N, Meissner G. Ca^{2+}-mediated activation of the skeletal-muscle ryanodine receptor ion channel. *J Biol Chem* 2018;**293**:19501–19509.
14. Chirasani VR, Xu L, Addis HG, Pasek DA, Dokholyan NV, Meissner G, Yamaguchi N. A central core disease mutation in the Ca^{2+}-binding site of skeletal muscle ryanodine receptor impairs single-channel regulation. *Am J Physiol Cell Physiol* 2019;**317**:C358–C365.
15. Zhang XH, Morad M. Calcium signaling in human stem cell-derived cardiomyocytes: evidence from normal subjects and CPVT afflicted patients. *Cell Calcium* 2016;**59**:98–107.
16. Zhang XH, Morad M. Ca^{2+} signaling of human pluripotent stem cells-derived cardiomyocytes as compared to adult mammalian cardiomyocytes. *Cell Calcium* 2020;**90**:102244.
17. de Juan-Sanz J, Holt GT, Schreiter ER, de Juan F, Kim DS, Ryan TA. Axonal endoplasmic reticulum Ca^{2+} content controls release probability in CNS nerve terminals. *Neuron* 2017;**93**: 867–881 e866.
18. Si-Tayeb K, Noto FK, Sepac A, Sedlic F, Bosnjak ZJ, Lough JW, Duncan SA. Generation of human induced pluripotent stem cells by simple transient transfection of plasmid DNA encoding reprogramming factors. *BMC Dev Biol* 2010;**10**:81.
19. Wei H, Zhang XH, Clift C, Yamaguchi N, Morad M. CRISPR/Cas9 gene editing of RyR2 in human stem cell-derived cardiomyocytes provides a novel approach in investigating dysfunctional Ca^{2+} signaling. *Cell calcium* 2018;**73**:104–111.
20. Zhang XH, Wei H, Xia Y, Morad M. Calcium signaling consequences of RyR2 mutations associated with CPVT1 introduced via CRISPR/Cas9 gene editing in human-induced pluripotent stem cell-derived cardiomyocytes: comparison of RyR2-R420Q, F2483I, and Q4201R. *Heart Rhythm* 2021;**18**:250–260.
21. Yamaguchi N, Zhang XH, Morad M. CRISPR/Cas9 gene editing of RYR2 in human iPSC-derived cardiomyocytes to probe Ca^{2+} signaling aberrancies of CPVT arrhythmogenesis. *Methods Mol Biol* 2022;**2573**:41–52.
22. Pahlavan S, Morad M. Total internal reflectance fluorescence imaging of genetically engineered ryanodine receptor-targeted Ca^{2+} probes in rat ventricular myocytes. *Cell calcium* 2017;**66**:98–110.
23. Zhang XH, Haviland S, Wei H, Šaric T, Fatima A, Hescheler J, Cleemann L, Morad M. Ca^{2+} signaling in human induced pluripotent stem cell-derived cardiomyocytes (iPS-CM) from normal and catecholaminergic polymorphic ventricular tachycardia (CPVT)-afflicted subjects. *Cell Calcium* 2013;**54**:57–70.
24. Haviland S, Cleemann L, Kettlewell S, Smith GL, Morad M. Diversity of mitochondrial Ca^{2+} signaling in rat neonatal cardiomyocytes: evidence from a genetically directed Ca^{2+} probe, mitycam-E31Q. *Cell Calcium* 2014;**56**:133–146.
25. Dark N, Cosson MV, Tsansizi LI, Owen TJ, Ferraro E, Francis AJ, Tsai S, Bouissou C, Weston A, Collinson L, Abi-Gerges N, Miller PE, MacLeod KT, Ehler E, Mitter R, Harding SE, Smith JC, Bernardo AS. Generation of left ventricle-like cardiomyocytes with improved structural, functional, and metabolic maturity from human pluripotent stem cells. *Cell Rep Methods* 2023;**3**:100456.
26. Marchiano S, Nakamura K, Reinecke H, Neidig L, Lai M, Kadota S, Perbellini F, Yang X, Klaiman JM, Blakely LP, Karbassi E, Fields PA, Fenix AM, Beussman KM, Jayabalu A, Kalucki FA, Potter JC, Futakuchi-Tsuchida A, Weber GJ, Dupras S, Tsuchida H, Pabon L, Wang L, Knollmann BC, Kattman S, Thies RS, Sniadecki N, MacLellan WR, Bertero A, Murry CE. Gene editing to prevent ventricular arrhythmias associated with cardiomyocyte cell therapy. *Cell Stem Cell* 2023;**30**:396–414 e399.
27. Cheng H, Smith GL, Hancox JC, Orchard CH. Inhibition of spontaneous activity of rabbit atrioventricular node cells by KB-R7943 and inhibitors of sarcoplasmic reticulum Ca^{2+} ATPase. *Cell calcium* 2011;**49**:56–65.
28. Wang L, Myles RC, Lee IJ, Bers DM, Ripplinger CM. Role of reduced sarco-endoplasmic reticulum Ca^{2+}-ATPase function on sarcoplasmic reticulum Ca^{2+} alternans in the intact rabbit heart. *Front Physiol* 2021;**12**:656516.
29. Peppiatt CM, Collins TJ, Mackenzie L, Conway SJ, Holmes AB, Bootman MD, Berridge MJ, Seo JT, Roderick HL. 2-Aminoethoxydiphenyl Borate (2-APB) antagonises inositol 1,4,5-trisphosphate-induced calcium release, inhibits calcium pumps and has a use-dependent and slowly reversible action on store-operated calcium entry channels. *Cell calcium* 2003;**34**:97–108.
30. Togashi K, Inada H, Tominaga M. Inhibition of the transient receptor potential cation channel TRPM2 by 2-aminoethoxydiphenyl borate (2-APB). *Br J Pharmacol* 2008;**153**:1324–1330.
31. Xu SZ, Zeng F, Boulay G, Grimm C, Harteneck C, Beech DJ. Block of TRPC5 channels by 2-aminoethoxydiphenyl borate: a differential, extracellular and voltage-dependent effect. *Br J Pharmacol* 2005;**145**:405–414.
32. Griffiths EJ. Use of ruthenium red as an inhibitor of mitochondrial Ca^{2+} uptake in single rat cardiomyocytes. *FEBS Lett* 2000;**486**:257–260.
33. Bai D, del Corsso C, Srinivas M, Spray DC. Block of specific gap junction channel subtypes by 2-aminoethoxydiphenyl borate (2-APB). *J Pharmacol Exp Ther* 2006;**319**:1452–1458.
34. Kondo RP, Weiss JN, Goldhaber JI. Putative ryanodine receptors in the sarcolemma of ventricular myocytes. *Pflugers Archiv Eur J Physiol* 2000;**440**:125–131.
35. Zhang XH, Wei H, Šarić T, Hescheler J, Cleemann L, Morad M. Regionally diverse mitochondrial calcium signaling regulates spontaneous pacing in developing cardiomyocytes. *Cell Calcium* 2015;**57**:321–336.
36. Marjamaa A, Laitinen-Forsblom P, Wronska A, Toivonen L, Kontula K, Swan H. Ryanodine receptor (RyR2) mutations in sudden cardiac death: studies in extended pedigrees and phenotypic characterization in vitro. *Int J Cardiol* 2011;**147**:246–252.
37. Shan J, Xie W, Betzenhauser M, Reiken S, Chen BX, Wronska A, Marks AR. Calcium leak through ryanodine receptors leads to atrial fibrillation in 3 mouse models of catecholaminergic polymorphic ventricular tachycardia. *Circ Res* 2012;**111**:708–717.
38. Sun B, Yao J, Ni M, Wei J, Zhong X, Guo W, Zhang L, Wang R, Belke D, Chen YX, Lieve KVV, Broendberg AK, Roston TM, Blankoff I, Kammeraad JA, von Alvensleben JC, Lazarte J, Vallmitjana A, Bohne LJ, Rose RA, Benitez R, Hove-Madsen L, Napolitano C, Hegele RA, Fill M, Sanatani S, Wilde AAM, Roberts JD, Priori SG, Jensen HK, Chen SRW. Cardiac ryanodine receptor calcium release deficiency syndrome. *Sci Transl Med* 2021;**13**:eaba7287.
39. Zhong X, Guo W, Wei J, Tang Y, Liu Y, Zhang JZ, Tan VH, Zhang L, Wang R, Jones PP, Napolitano C, Priori SG, Chen SRW. Identification of loss-of-function RyR2 mutations associated with idiopathic ventricular fibrillation and sudden death. *Biosci Rep* 2021;**41**: BSR20210209.
40. Morad M, Zhang XH. Mechanisms of spontaneous pacing: sinoatrial nodal cells, neonatal cardiomyocytes, and human stem cell derived cardiomyocytes. *Can J Physiol Pharmacol* 2017;**95**: 1100–1107.
41. De Smet MAJ, Lissoni A, Nezlobinsky T, Wang N, Dries E, Pérez-Hernández M, Lin X, Amoni M, Vervliet T, Witschas K, Rothenberg E, Bultynck G, Schulz R, Panfilov AV, Delmar M, Sipido KR, Leybaert L. Cx43 hemichannel microdomain signaling at the intercalated disc enhances cardiac excitability. *J Clin Invest* 2021;**131**:e137752.